Long-term evolution of terrestrial inputs from the Ediacaran to early Cambrian: clues from Nd isotopes in shallow-marine carbonates, South China

Guang-Yi Wei[1]*, Hong-Fei Ling[1]*, Graham A. Shields[2], Tianyu Chen[1], Maxwell Lechte[3], Xi Chen[1], Chen Qiu[1], Huanling Lei[1], Maoyan Zhu[4]

[1]State Key Laboratory for Mineral Deposits Research, Department of Earth Sciences, School of Earth Sciences and Engineering, Nanjing University, 163 Xianlin Avenue, Nanjing 210023, China.

[2]Department of Earth Sciences, University College London, Gower Street, London WC1E 6BT, U.K.

[3]School of Earth Sciences, University of Melbourne, Parkville, Victoria 3010, Australia

[4]State Key Laboratory of Palaeobiology and Stratigraphy, Nanjing Institute of Geology and Palaeontology, Nanjing 210008, China.

* Corresponding author

E-mail address: guangyiwei@nju.edu.cn; wgynjues@gmail.com (Guang-Yi Wei); hfling@nju.edu.cn (Hong-Fei Ling).

Abstract

The emergence and radiation of metazoans have been widely attributed to a progressively more oxidizing surface environment through the Ediacaran–Cambrian transition interval. However, the root causes for atmospheric and oceanic oxygenation are still disputed. Long-term tectonic changes could possibly have led to atmospheric oxygenation but geochemical evidence for this linkage remains elusive. In this study, we analyzed the radiogenic Nd isotopic compositions (εNd) of shallow-marine carbonates from South China in order to track secular variations in terrestrial inputs from Ediacaran to early Cambrian time. Compared with most other geochemical indices, the Nd isotope system in carbonates is less susceptible to early diagenetic exchange and can thus act as a robust proxy for continental materials undergoing weathering. We interpret an abrupt excursion to lower εNd values during the middle Ediacaran as due to rapid exchange of different water masses. However, the more gradual trend towards lower εNd values from the Ediacaran to early Cambrian, accompanied by increasing $^{87}Sr/^{86}Sr$ ratios of the studied carbonates, likely indicates the enhanced weathering of old continental rock following the assembly of Gondwana. Increased net accumulation of atmospheric oxygen as a result of enhanced organic carbon burial may have benefited from intense continental denudation.

Keywords: neodymium isotope record; continental denudation; tectonic activity; Neoproterozoic oxygenation event; animal radiation

1. Introduction

The Neoproterozoic Era (1000 Ma to ~ 540 Ma) witnessed the emergence of metazoans and modern ecosystems (Sperling et al., 2013; Knoll and Nowak, 2017), accompanied by a fundamental baseline rise in Earth-surface oxygen levels (Canfield et al., 2007; Och and Shields-Zhou, 2012; Lyons et al., 2014). Nevertheless, oceanic redox conditions underwent dynamic fluctuations with several oxygenation episodes of an overall anoxic ocean are proposed for the late Neoproterozoic (Wood et al., 2015; Sahoo et al., 2016; Wei et al., 2018; Zhang et al., 2018). In addition to uncertainties around the trajectory of redox evolution, the triggers for atmospheric and oceanic oxygenation are also disputed. More effective oxygenic photosynthesis by eukaryotic algae was commonly considered to have produced more oxygen in the late Neoproterozoic (e.g., Brocks et al., 2017) while the net accumulation of oxygen is also determined by the changing consumption of oxygen by reductants. Tectonic controls on Earth-surface oxygenation have also been invoked in previous research (e.g., Kump and Barley, 2007; Campbell and Allen, 2008; Lee et al., 2016; Planavsky, 2018; Li et al., 2018) although tectonic drivers have not been comprehensively demonstrated by geochemical records. In particular, variations in continental denudation as well as global oceanic circulation following Gondwana amalgamation from the middle Ediacaran to early Cambrian are not well constrained.

Initial radiogenic Nd isotope composition of ancient seawater recorded by marine carbonates (defined as $\varepsilon Nd(t)$, relative to Chondritic Uniform Reservoir, CHUR) can be an effective tracer of terrestrial inputs to epeiric seas and ocean basins. Dissolved Nd in the ocean is dominantly derived from the weathering of terrestrial rocks (Piepgras and Wasserburg, 1985; Goldstein and Jacobsen, 1987) with additional inputs such as dust, groundwater and seafloor sediment (Frank, 2002; Lacan and Jeandel, 2004; Lacan et al., 2012). Due to its short oceanic residence time (~600 yr) compared with the mixing time scales of the global ocean, the Nd isotopic compositions have shown considerable variability in the modern oceans (Tachikawa et al., 2017). The high spatial variability of present-day εNd in the modern ocean is closely linked with various weathered Nd sources to different water-mass and global deep-ocean circulation (Albarède and Goldstein, 1992; Goldstein and Hemming, 2014). Deep North Atlantic water has a significantly lower εNd value (~ –13.5) due to riverine input from weathered old continental crust. By contrast, the Pacific ocean, which is surrounded by juvenile magmatic arcs, generally has a comparatively higher εNd value (~ –4). εNd values of Indian intermediate and deep water are around –8, due to the advection of seawaters from the Circum-Antarctic Current (Goldstein and Hemming, 2014). The great spatial variability of εNd in the global ocean is determined by the heterogeneity of weathered Nd sources to different water-mass and global deep-ocean circulation (Albarède and Goldstein, 1992; Goldstein and Hemming, 2014). Irrespective of spatial heterogeneities in modern global seawater εNd values, temporal εNd(t) variations in ancient epeiric water bodies, recorded by marine sediments in a certain area, are also considered to be controlled by fluctuations in sea level (Grandjean et al., 1988; Holmden et al., 1998). Therefore, temporal variations in εNd(t) values of continental shelf seawater generally depend on changes in the weathering source and the degree of water-mass exchange with the more open ocean.

In this study, we present new, high-resolution radiogenic Nd isotope data for shallow-marine carbonates from the Jiulongwan–Gaojiaxi–Yanjiahe section, South China to reconstruct shallow seawater εNd(t) evolution on the continental shelf margin of the Yangtze block from the Ediacaran to early Cambrian. Neodymium isotopic compositions, combined with radiogenic Sr isotope ratios, are used to directly track the terrestrial inputs and oceanic circulation during this interval. These new data help to constrain the evolution of marine environment on continental shelves and offer valuable insights into the potential correlation of continental denudation and tectonic activity, and their links to atmospheric oxygenation and the emergence of complex metazoans.

2. Geological setting

The Doushantuo Formation of the Jiulongwan section in the Yangtze Gorges area is the product of sedimentation in a shallow seawater environment, at or below wave base in an inner shelf lagoon setting (Jiang et al., 2011). At the Jiulongwan section, the Doushantuo Formation has been divided into four members. Member I is an approximately 5-m-thick ‘cap dolostone’ featuring a zircon U-Pb age of 635.2 $\pm$0.6 Ma (Condon et al., 2005), overlying the Nantuo glacial diamictite. Member II is ca. 70 m thick and consists of alternating organic-rich black shale and dolostone bed with pea-sized cherty nodules. Member III comprises about 50-m-thick dolostone variably interbedded with chert in the lower part and limestone in the upper part. Member IV is a ~ 10 m thick black shale, also known as the ‘Miaohe member’ in other localities in the Yangtze Gorges area (e.g., Jiang et al., 2011).

The Dengying Formation of the Gaojiaxi section is characterized by relatively pure carbonates overlying the Doushantuo Formation, with a zircon U-Pb age 551 $\pm$0.7 Ma at its base (Condon et al., 2005). The Dengying Formation in the studied area, can be divided into three members: the basal Hamajing Member, the middle Shibantan Member and the uppermost Bamatuo Member. The Hamajing Member is ca. 21 m thick and consists of intraclastic and oolitic dolomitic grainstone. The Shibantan Member consists of dark gray thin- to intermediate-bedded micritic limestone with a total thickness of ca. 50 m and contains Ediacara-type fossils (e.g., Chen et al., 2014). The Bamatuo Member is ca. 40 m thick and consists of micritic and sparitic dolostones.

The 54-m-thick Yanjiahe Formation of the Yanjiahe section is characterized by two sub-cycles of shoaling. The lower sub-cycle (~ 29 m) consists of dark grey laminated dolostone interbedded with cherty dolostone, siliceous layers with black shale, and dolostone containing cherty and phosphatic clasts. The upper sub-cycle (~ 25 m) is characterized by black chert with laminated black shale, laminated limestone interbedded with black shale, and limestone with siliceous and phosphate. The Yanjiahe Formation yields early Cambrian Small Shelly Fossil Assemblage Zone 1 (SS1) in the dolostone layer with phosphatic clasts and Small Shelly Fossil Assemblage Zone 3 (SS3) in the upper phosphatic limestone (Jiang et al., 2012). The Ediacaran-Cambrian boundary is considered to be at the bottom of the lower dolostone layer where the SS1 first occurs (Chen, 1984).

3. Materials and methods

We analyzed 75 bulk carbonate samples collected from the Doushantuo Formation, Dengying Formation and Yanjiahe Formation from the Jiulongwan–Gaojiaxi–Yanjiahe section, Yangtze Gorges area, Hubei Province, South China (Fig. 1). As reported previously (Ling et al., 2013; Wei et al., 2018, 2019), the best-preserved and least-contaminated carbonate samples primarily composed of micritic dolomite or calcite were selected and drilled for geochemical analyses.

3.1 Neodymium isotope analyses

For Nd isotope analysis, a two-step leaching method was used to dissolve the marine carbonate component from the bulk samples which may contain other minor components (cf. Bailey et al., 2000; Li et al., 2011; Tissot et al., 2018). Approximately 200 mg powder was firstly rinsed with MQ ultra-pure water, and then leached with 3 ml 0.5 N double-distilled acetic acid (HAc) for 4 hours in order to remove possible contaminants added after marine carbonate deposition. This leachate was discarded after centrifugation, and the insoluble residue was rinsed and centrifuged three times with MQ water. Then 5 ml 1 N double-distilled HAc was added to leach the residue for 4 hours, after which the leachate solution was collected and dried, and then re-dissolved in 5 ml 6 N HCl in preparation for Nd extraction. A two-step resin column method was used for Nd separation and purification (modified after Hirahara et al., 2012). The first elution discards the matrix ion (such as K, Na, Ca, Mg, Sr) from the sample solution, using Bio-rad AG50W-X8 (200-400 mesh) cation resin. The second elution separates Nd from the other rare earth elements (REE), using Eichrom Ln specific resin. The resultant pure Nd solution was dried, and then re-dissoloved in 3% HNO_3 for isotopic analyses.

Nd isotope analyses were performed on a Thermo Neptune Plus Multicollector, Inductively-Coupled Plasma Mass Spectrometer (MC-ICP-MS) at the State Key Laboratory for Mineral Deposits Research, Nanjing University, and a Nu Plasma II MC-ICP-MS at Nanjing FocuMS Technology Co. Ltd (www.focums.com). $^{143}Nd/^{144}Nd$ ratios were normalized to a $^{146}Nd/^{144}Nd$ ratio of 0.7219 in order to correct for mass fractionation during analysis. United States Geological Survey standards BRC-2, AGC-2 and BHVO-2 were also digested and analyzed during this study in order to monitor the analytical precision; their $^{143}Nd/^{144}Nd$ values were measured at 0.512636 $\pm$0.000002, 0.512797 $\pm$0.000002 and 0.512986 $\pm$0.000002 (SE), respectively.

The studied carbonates are divided into five intervals, with suggested mean depositional ages as follows: ~ 635 Ma for Doushantuo Member I, ~ 580 Ma for Doushantuo Member II, ~ 565 Ma for Doushantuo Member III, ~ 545 Ma for Dengying Formation and ~ 535 Ma for Yanjiahe Formation (age estimates from Condon et al., 2005; Jiang et al., 2012). $^{143}Nd/^{144}Nd$ ratios were corrected for production of ^{143}Nd from ^{147}Sm decay since the time of deposition of the carbonates, and reported as initial εNd(t) (hereafter termed εNd(t)) relative to $^{143}Nd/^{144}Nd$ ratios of CHUR at time of deposition (present $^{143}Nd/^{144}Nd$ = 0.512638 and $^{147}Sm/^{144}Nd$ = 0.1967, Jacobsen and Wasserburg, 1980). The initial $^{143}Nd/^{144}Nd$ ratios of samples are calculated by following equations:

$$^{143}Nd/^{144}Nd(t) = {}^{143}Nd/^{144}Nd(0) - {}^{147}Sm/^{144}Nd(0) \times (e^{\lambda t} - 1) \quad (1)$$

$$^{147}Sm/^{144}Nd(0) = ([Sm]/A_{Sm} \times [^{147}Sm_{natural}]) \;/\; ([Nd]/A_{Nd} \times [^{144}Nd_{natural}]) \quad (2)$$

whereby $^{143}Nd/^{144}Nd(t)$ is the $^{143}Nd/^{144}Nd$ ratio of the carbonate when it was deposited; $^{143}Nd/^{144}Nd(0)$ is the $^{143}Nd/^{144}Nd$ ratio we analyzed in the lab; λ is the decay constant of ^{147}Sm ($\lambda = 6.54 \times 10^{-12}$, Lugmair and Marti, 1978); t is the age of carbonates in this study; [Sm] and [Nd] is Sm and Nd concentrations of the carbonate, measured using a Thermo Element-II ICP-MS at the State Key Laboratory for Mineral Deposits Research, Nanjing University; A_{Sm} and A_{Nd} are atomic weights of Sm (150.36) and Nd (144.242) (Meija et al., 2016); $^{147}Sm_{natural}$ and $^{144}Nd_{natural}$ are natural abundance of Sm (0.1499) and Nd (0.23798) (Berglund and Wieser, 2011). The initial $^{143}Nd/^{144}Nd$ of studied carbonate is presented as $\varepsilon Nd(t)$ here, defined by:

$$\varepsilon Nd(t) = [^{143}Nd/^{144}Nd(t)_{sample} \;/\; {}^{143}Nd/^{144}Nd(t)_{CHUR} - 1] \times 10000 \quad (3)$$

$$^{143}Nd/^{144}Nd(t)_{CHUR} = {}^{143}Nd/^{144}Nd(0)_{CHUR} - {}^{147}Sm/^{144}Nd(0)_{CHUR} \times (e^{\lambda t} - 1) \quad (4)$$

Whereby t is the same time as deposition of the studied carbonate, $^{143}Nd/^{144}Nd(0)_{CHUR}$ = 0.512638, and $^{147}Sm/^{144}Nd(0)_{CHUR}$ = 0.1967 (Jacobsen and Wasserburg, 1980).

3.2 Strontium isotope analyses

For Sr isotope analysis, a two-step leaching method was also used to dissolve the marine carbonate component from the bulk samples (see Bailey et al., 2000; Li et al., 2011 for details). Sr isotope ratios were determined with a Thermo Tritium MC-TIMS at the State Key Laboratory for Mineral Deposits Research, Nanjing University. Long-term reproducibility of the analyses was detected by repeated measurement of Sr isotope standard NIST SRM 987 with an average value of 0.710252 ($\pm$0.000016).

3.3 Carbon and oxygen isotope analyses

Carbon and oxygen isotopes of the carbonate samples in this study were analyzed using a Finnigan Gasbench II online analysis system + Delta Plus XP mass spectrometer at the State Key Laboratory for Mineral Deposits Research, Nanjing University. The results of C and O isotope are presented relative to V-PDB. External precision for C and O isotope analyses is 0.06‰ (2SD) and 0.07‰ (2SD), respectively, based on repeated measurements of the Chinese GBW00405 carbonate standard (referred $\delta^{13}C = 0.57 \pm 0.03‰$; $\delta^{18}O = -8.49‰ \pm 0.14‰$).

4. Results

Results of radiogenic Nd isotope ratio (reported as εNd(t)) , Nd concentration and radiogenic Sr isotope ratio in this study as well as published C isotope data (Ling et al., 2013) are shown in Figure 2 and Supplementary Table 1.

Cap dolostones (i.e. the Doushantuo Member I) in the Jiulongwan section yield relatively high εNd(t) values from –5.86 to –2.91 as well as high Nd concentrations from 1.45 ppm to 5.67 ppm. $^{87}Sr/^{86}Sr$ ratios in cap dolostones range from 0.7083 to 0.7123 (data from Wei et al., 2019). Carbonates in the Doushantuo Member II have slightly lower εNd(t) values than cap dolostones, ranging from –6.83 to –2.73. Nd concentrations of the carbonates in this member range from 0.96 to 9.28 with some scatter. $^{87}Sr/^{86}Sr$ ratios of the carbonates in this member are relatively stable, ranging from 0.7079 to 0.7087. Carbonates in the Doushantuo Member III record significantly low εNd(t) values from –10.9 to –7.38 with Nd concentrations between 2.74 and 7.70 ppm (except for a very low value of 0.81). $^{87}Sr/^{86}Sr$ ratios of the carbonates in the Doushantuo Member III are relatively consistent and overall higher than those in the Member II, ranging from 0.7084 to 0.7095.

Carbonates of the Dengying Formation in the Gaojiaxi–Yanjiahe section record relatively consistent εNd(t) values and Nd concentrations. Most εNd(t) values of the carbonates in the Dengying Formation rang from –7.35 to –4.92 except for one low point (–8.79, sample WH-1), which are slightly higher than those in the Doushantuo Member III, but appreciably lower than those in the Doushantuo Member I and slightly lower than those in the Doushantuo Member II. Neodymium concentrations of the carbonates in the Dengying Formation are significantly lower than those in the Doushantuo Formation and range from 0.10 ppm to 1.77 ppm except for four points higher than 3 ppm. $^{87}Sr/^{86}Sr$ ratios of the carbonates in the Dengying Formation are slightly lower than those in the Doushantuo Member III, ranging from 0.7084 to 0.7092.

Carbonates in the Yanjiahe Formation yield lower εNd(t) values and elevated Nd concentrations, relative to carbonates in the Dengying Formation. εNd(t) values of the carbonates in this formation range from –8.90 to –7.16 except for one relatively high point (-3.99, sample YJH-30) and Nd concentrations generally range from 0.36 to 14.40 ppm with some scatter. $^{87}Sr/^{86}Sr$ ratios in the Yanjiahe Formation are higher than those in the Dengying Formation, ranging from 0.7086 to 0.7097.

5. Discussion

5.1 Effects of silicate detritus and diagenetic alteration on carbonate εNd(t)

Rare earth elements and yttrium (REY) in shallow marine carbonates are susceptible to detrital contamination due to significantly higher REY contents in silicate detritus than in carbonate minerals and the potentially high clastic sedimentation rates of shallow marine settings. A part of silicate-associated REY could be transferred into the carbonate component during diagenesis or be leached from the silicate fraction during sample preparation. For example, the Nd isotopic compositions of deep marine authigenic sediments have been shown to covary with those of detrital inputs, resulting from late burial diagenesis (e.g., Du et al., 2016; Jang et al., 2018). Because aluminum (Al) and thorium (Th) concentrations are high in silicate minerals but exceedingly low in seawater, covariation between Al and/or Th and other elements or isotope values is widely used to detect detrital silicate contamination of measured carbonate Nd isotope values (e.g., Webb and Kamber, 2000; Ling et al., 2013; Zhao and Zheng, 2014, 2017; Wei et al., 2018, 2019). Leached carbonate components of the samples in this study show significantly low Al (< 0.2%) and Th concentrations (< 1 ppm) and exhibit no clear covariations between Nd or εNd(t) and Al or Th concentrations (Fig. 3), which suggests only negligible influence from silicate detritus on Nd content and Nd isotope data in this study. To further check the impact of detrital silicate-associated Nd on leachate Nd isotope values, we use the following equations to calculate Nd concentrations and εNd(t) values of the pure carbonate component by subtracting possible contributions from silicate detritus, assuming that the Al contents of the bulk carbonatesoriginated from silicate detritus.

$$[Nd]_{det} = [\frac{Nd}{Al}]_{det} \times [Al]_{bulk} \qquad (4)$$

$$[Nd]_{carb} = [Nd]_{bulk} - [Nd]_{det} \quad (5)$$

$$\varepsilon Nd(t)_{carb} = (\varepsilon Nd(t)_{bulk} \times [Nd]_{bulk} - \varepsilon \mathrm{Nd(t)}_{det} \times [Nd]_{det}) \,/\, [Nd]_{carb} \quad (6)$$

whereby $[Al]_{bulk}$, $[Nd]_{bulk}$, $\varepsilon Nd(t)_{bulk}$ represent the measured concentrations of Al, Nd, and Nd isotope value, respectively, for each sample using the two-step leaching method (see the result section and supplementary table for details); $[Nd/Al]_{det}$ and $\varepsilon Nd(t)_{det}$ are Nd/Al ratio and Nd isotope value of terrestrial detritus contained in carbonate, which are assumed to equal those of Post-Archean Australian Shale (PAAS) (Nd/Al = 3.7, εNd(t) = –12) (Taylor and McLennan, 1985, Allègre, 2008); $[Nd]_{det}$ is the calculated Nd concentration contributed from the detritus to the sample leached solution; $[Nd]_{carb}$ and $\varepsilon Nd(t)_{carb}$ are calculated Nd concentration and $\varepsilon Nd(t)$ value of pure carbonate after detritus correction. The corrected $[Nd]_{carb}$ and $\varepsilon Nd(t)_{carb}$ values of pure carbonates, presented in Fig. 4, typically do not show large differences from the gross values analyzed from the bulk carbonates before correction, except for 4 samples (from 4 members/formations) whose $\varepsilon Nd(t)_{carb}$ values represent outliers, being significantly higher than their gross values (Figs. 4 and 5). This suggests possible overcorrection of these 4 samples and so they are not considered further. Meanwhile, no clear correlations of $\varepsilon Nd(t)_{bulk}$ vs. $[Nd]_{bulk}$ and $\varepsilon Nd(t)_{carb}$ vs. $[Nd]_{carb}$ are observed (Fig. 5A and B). Hence, carbonate samples in this study can reflect the geochemical information of contemporaneous seawater without significant contamination from continental silicate detritus contained in the bulk carbonate samples.

In addition to terrestrial silicate detritus, early diagenetic processes may alter the elemental and isotopic compositions of shallow marine carbonates (Ohelert and Swart, 2014; Higgins et al., 2018; Stewart et al., 2015; Chen et al., 2018). However, marine carbonate REY are more likely less sensitive to diagenetic processes, potentially benefiting from high partition coefficients for REY during the carbonate mineral precipitation from seawater, or from usually very low concentrations of REY in low temperature fluids (e.g., Webb and Kamber, 2000; Webb et al., 2009; Zhao and Zheng, 2014, 2017). Even in modern meteoric and marine diagenetic zone (e.g., Great Bahama Bank), marine carbonates were demonstrated to record primary seawater REY signatures (Liu et al., 2019). Additionally, marine dolomitization has been proposed to have a negligible effect on the retention of initial seawater REE signatures in primary carbonates (Nothdurft et al., 2004; Bau and Alexander, 2006). Lack in correlations of $[Nd]_{carb}$ vs. Mg/Ca and $\varepsilon Nd(t)_{carb}$ vs. Mg/Ca (Fig. 5C and D) likewise supports that variations in $[Nd]_{carb}$ and $\varepsilon Nd(t)_{carb}$ of the carbonates in this study are not driven by early diagenetic dolomitization. In conclusion, the Nd isotopic compositions of marine carbonates are proposed to behave conservatively during early diagenesis, which is conducive to the use of Nd isotopes of shallow-marine carbonates as a paleoenvironmental proxy.

5.2 Fluctuations of εNd(t) in continental shelf seawater recorded in carbonates from the Ediacaran to early Cambrian

Seawater εNd(t) recorded by carbonate rocks from Yangtze Gorges area, South China in this study show three significant excursions to lower values from the early Ediacaran to early Cambrian (N1, N2, N3 in Fig. 4D). These εNd(t) excursions are interestingly coincident with the negative $\delta^{13}C$ excursions in the Doushantuo Member I (N1), Doushantuo Member III (N2) and Yanjiahe Formation (N3), respectively (Fig. 2A). Generally, abrupt changes in seawater εNd(t) are considered to have been driven by changes in seawater circulation and continental weathering inputs, likely controlled by global climate change and long-term tectonic activity (e.g., Goldstein and Hemming, 2014; Dera et al., 2015). However, studies of carbonates deposited in continental shelf waters suggest that εNd(t) values in those environments may also depend on paleoceanographic position and sea-level fluctuations, reflecting variations in local terrestrial flux to the continental shelf (Fanton et al., 2002; Holmden et al., 2013; Dopieralska et al., 2016). Hence, we suggest that secular εNd(t) variations of the shallow-marine carbonates in this study are primarily caused mainly by changes in Nd source and flux associated with terrestrial input or water-mass exchange. In the context of a marine sedimentary environment for the Yangtze block from the Ediacaran to early Cambrian, Nd isotopic compositions of the Yangtze shelf seawater is dominated by weathered materials from adjacent continental blocks as well as ocean currents with distinct εNd(t) values.

To track the potential effect of continental denudation on εNd(t) values of continental shelf seas, εNd(t) data for marine carbonates in this study are compared with those of Neoproterozoic clastic sedimentary rocks sourced from terrestrial silicate detritus (Fig. 6A). Relatively high εNd(t) values (> –3) of the clastic rocks suggest extensive weathering of mafic rocks prior to the Ediacaran Period, which is consistent with the emplacement of large igneous provinces (LIP's) (rapid extrusion of huge volume of mafic volcanic rocks in less than several million years) during the early Neoproterozoic (Fig. 6A, Cox et al., 2016 and references therein). Compilations of εNd(t) values from Neoproterozoic mudstone, diamictite and iron formation display a decreasing trend from the late Cryogenian to the Ediacaran period (Fig. 6A), suggesting an increasing influence from the weathering of crystalline crustal basement (e.g., Cox et al., 2016). εNd(t) values of shallow-marine carbonates from South China in this study vary in step with the overall trend of εNd(t) in clastic rocks, more likely controlled by secular changes in relative proportions of felsic versus mafic rock weathering (Fig. 6A). However, superimposed on this long-term global trend, the three negative εNd(t) excursions with distinct εNd(t) values from the Ediacaran to early Cambrian (Fig. 4D) may have resulted from relatively short-term changes in the εNd(t) compositions of continental shelf seawater, in response to local-to-regional environmental changes (see discussion below).

5.2.1 εNd(t) variations in the Marinoan cap dolostone

The Marinoan cap dolostones in this study have relatively high εNd(t) values (average εNd(t) = –3.94) as well as an appreciable negative εNd(t) excursion in its lower part (lowest to -5.72) (Fig. 4D). The average εNd(t) value of cap dolostones is very close to that of the modern Pacific Ocean (εNd(t) = –4, Goldstein and Hemming, 2014), and we suggest this is an inherited εNd(t) signature from the syn-glacial Cryogenian ocean (Cox et al., 2016; Gernon et al., 2016). In the context of a short duration for cap dolostone deposition (e.g. Shields, 2005; Hoffman et al., 2017), synsedimentary dolomitization in a brackish mixture of freshwater and seawater has been proposed as a mechanism for cap dolostone deposition, which could explain the dramatic Ca and radiogenic Sr isotope excursions in the lower cap dolostone succession (Wei et al., 2019). The rapid change in εNd(t) could similarly have been influenced by mixing of isotopically distinct water bodies in the aftermath of the end-Cryogenian 'Marinoan' glaciation. The abrupt addition of abundant fresh meltwater (from rivers and groundwater) into continental shelf areas could have rapidly decreased carbonate εNd(t) values because freshwater generally has significantly higher Nd concentrations, with less radiogenic Nd, relative to the open oceans (Goldstein and Jacobsen, 1987). Compared with the $^{87}Sr/^{86}Sr$ system, which is sensitive to differential weathering of Rb-rich silicate minerals in the post-glaciation (Blum and Erel, 1995; Prestrud Anderson et al., 1997; Li et al., 2007), the $^{143}Nd/^{144}Nd$ system is relatively less susceptible to incongruent weathering of different silicate minerals (Bayon et al., 2015). Hence, overall the Doushantuo cap dolostones record high εNd(t) values of continental shelf seawater in the aftermath of the Marinoan glaciation, despite a perceptible negative excursion at the base.

Relatively high average εNd(t) values (~ –4) and low $^{87}Sr/^{86}Sr$ ratios (~ 0.7080) of the carbonates from Doushantuo Member II indicate that the weathering of juvenile magmatic rock dominated riverine inputs into continental shelf seawater (cf. modern Pacific Ocean) throughout deposition of this Member (Fig. 4D). A relatively high proportion of Nd derived from juvenile rocks likely relates to the protracted breakup of the Rodinia supercontinent into the early Ediacaran (Li et al., 2013), suggesting a secular tectonic control on εNd(t) composition of the continental shelf seawater.

5.2.2 Significantly negative εNd(t) excursion during the Shuram Excursion

Carbonates of the Doushantuo Member III in this study are characterized by extremely low $\delta^{13}C$ values (lowest to –10‰), which can be correlated to the Shuram negative $\delta^{13}C$ excursion (or DOUNCE) (McFadden et al., 2008; Lu et al., 2013). This widespread $\delta^{13}C$ excursion has been proposed to reflect either a primary marine signal or the product of secondary alteration, both of which suggest global environmental extremes during this period (e.g., Grotzinger et al., 2011). εNd(t) values recorded in these carbonates from South China exhibit a dramatic negative excursion (Fig. 4D) in step with the $\delta^{13}C$ variation (Fig. 2A). The average εNd(t) value for carbonates in Doushantuo Member III (–9.34) approaches the εNd(t) value of modern circum-Antarctic seawater (–8 to –9) (Piepgras and Wasserburg, 1982), which is much lower than the average values for the cap dolostone (–3.94) and Doushantuo Member II (–3.78).

A prolonged and large negative εNd(t) excursion could be caused by a change in continental weathering, exchange between seawater and shelf sediment or a change in ocean circulation (e.g., Zheng et al., 2013). Exchange between seawater/authigenic carbonate and seafloor sediment during late diagenesis has been suggested to alter Nd isotope signatures of local bottom waters or sediments, controlled by compositions of deeply buried sediments (Lacan and Jeandel, 2004; Abbott et al., 2016; Jang et al., 2018). However, the remobilization of seafloor surface sediments could only affect the εNd(t) composition of deep or intermediate seawater rather than shallow seawater (Lacan and Jeandel, 2004), which seems unlikely to contribute significantly to the negative εNd(t) excursion in Doushantuo Member III carbonates. Moreover, exchange between seawater and seafloor sediment would result in an appreciable correlation between εNd(t) values and Nd concentrations in the carbonate, as detrital sediments on seafloor and sedimentary pore water have significantly higher Nd concentrations, relative to bottom seawater (e.g., Abbott et al., 2016). Carbonates in this study exhibit no clear covariation between εNd(t) values and Nd concentrations (Fig. 5A and B), suggesting little contamination on shallow seawater εNd(t) from dissolution of detrital sediments. The elevated Nd concentrations of the carbonates during this period is more likely caused by the transition from the dolomite to calcite in this stratigraphic interval as calcite generally has much higher Nd concentration relative to dolomite and aragonite (e.g., Webb and Kamber, 2000; Webb et al., 2009). Hence, εNd(t) values of shallow seawater in this study are more likely controlled by the source and flux of Nd imported into the Yangtze margin area, regardless of the nature of early and late diagenetic alteration (e.g., Holmden et al., 1998; Dopieralska et al., 2016; Tachikawa et al., 2017). A previous study suggested that the negative εNd(t) excursion in the middle Ediacaran was induced by extensive weathering of more mature detritus from the Archean Kongling complex in the Yangtze block (Hu et al., 2016). However, this may meet difficulty when considering the subsequent increase of εNd(t) in the late Ediacaran (i.e., Dengying Formation) since weathering of the Kongling complex would have not been rapidly terminated as the Gondwana assembly was still in the process. Moreover, in view of a submarine sedimentary environment for the Yangtze area in the Ediacaran (Jiang et al., 2011), Nd in the Yangtze marginal seawater is more likely from weathered materials of adjacent exposed continental cratons, rather than only from those of the old terrain in the Yangtze block.

Although the age of the Shuram Excursion is not well constrained, the onset of this negative $\delta^{13}C$ excursion is considered to be later than the Gaskiers glaciation (~ 580 Ma, Pu et al., 2016) and previous studies have favoured a 9–10 Myr duration (Condon et al., 2005; Narbonne et al., 2012; Gong et al., 2017; Minguez et al., 2017; Wang et al., 2017). Therefore, the estimated age of the Shuram Excursion is believed to be broadly coincident with the early Gondwana assembly (cf.

Li et al., 2013). Paleo-continental reconstructions suggest that South China was isolated in low-middle latitudes and adjacent to Australia in Gondwana (Li et al., 2008, 2013; Xu et al., 2013; Zhao et al., 2018). εNd(t) values of carbonates from South China approach those of continental detrital sedimentary rocks from Australia (Fig. 6A). Thus, the decreased εNd(t) values of shallow marine carbonates generally may have resulted from enhanced continental weathering of old continental crust exposed during the early assembly process of Gondwana. In this point, the prominently negative εNd(t) excursion during the Shuram Excursion may have been driven by increased export of the weathered old continental felsic rocks to the adjacent seawater accompanying with the initial Gondwana assembly, which alters the preceding local seawater εNd(t) balance.

However, εNd(t) values of the carbonates in the Dengying Formation (~ –5) are much higher than those in the Doushantuo Member III and more similar to those in Doushantuo Member II (Fig. 4D). The elevated εNd(t) values in the Dengying Formation are considered to reflect an abrupt decrease in terrestrial inputs after the Shuram Excursion, which is unlikely interpreted by tectonic evolution due to the prolonged assembly of Gondwana during this period. This observation proposed that the dramatic εNd(t) anomaly during the Shuram Excursion may have been influenced by other factors in addition to variability in continental denudation. The detrital sediments in NW Laurentia have much lower εNd(t) values (< –15), compared with detrital sediments in other blocks, and show a similar trend in εNd(t) with carbonate εNd(t) record in the middle Ediacaran this study (Fig. 6A). Despite the protracted decrease in εNd(t) from the Neoproterozoic to the early Cambrian, an abrupt εNd(t) fall in detrital sediments of NW Laurentia is also observed in the middle Ediacaran, after which εNd(t) values in NW Laurentia increase slightly and approach to those of Australia (Fig. 6A). Given the observed εNd(t) variation in detrital sediments from NW Laurentia, the dramatically negative εNd(t) anomaly during the Shuram Excursion in this study may have been induced by exchange of seawater between South China and NW Laurentia due to intensified oceanic circulation and/or improved ocean connectivity during the middle Ediacaran. In this regard, water-mass exchange between South China and Laurentia may have been relatively rapid due to the opening gateway between these two cratons via the Mawson ocean (e.g., Li et al., 2013; Zhao et al., 2018). Further, global cooling in the middle Ediacaran (i.e., Gaskiers glaciation typically found on Laurentia, Hoffman and Li, 2009; Pu et al., 2016) may have accelerated the export of bottom seawater from high-latitude Laurentia to relatively low-latitude South China (cf. Zheng et al., 2013, 2016).

In conclusion, the abrupt low εNd(t) values of shallow-marine carbonates in the Doushantuo Member III, South China suggest an enhanced weathering of old continental rocks in step with more vigorous exchange of different water-masses, potentially driven by both tectonic activity and climate change. In the view of this, the elevated εNd(t) values in the Dengying Formation is more likely induced by recession of water mass mixing between South China and Laurentia, following the subsequent assembly of Gondwana. Additionally, εNd(t) anomaly in the middle Ediacaran Period interestingly coincides with negative C isotope excursion. Incorporation of such bottom water mass containing probably DOC to the shallow water mass in South China could have also contribute to the negative C isotope excursion of Shuram Excursion although other contributions may have also played roles in the light carbon isotope record. More research is needed to unravel the potential links between these two isotope systems during this period.

5.2.3 Decreased εNd(t) values of shallow carbonates in the early Cambrian

εNd(t) values of the carbonates in the Dengying Formation are relatively consistent and much higher than those in Doushantuo Member III. Considering that the abrupt negative εNd(t) anomaly in Doushantuo Member III reflects rapid transport of Laurentia-sourced seawater during the middle Ediacaran, we attribute the slight εNd(t) decrease in the Dengying Formation (–5.27 on average), relative to the Doushantuo Member II (–3.78 on average), to successive Gondwana assembly in the terminal Ediacaran (Fig. 4D).

Carbonates in the Yanjiahe Formation in this study have a relatively low average εNd(t) value (–7.33), compared with carbonates in the Dengying Formation (average εNd(t) = –5.27). The decrease in marine carbonate εNd(t) values from the terminal Ediacaran to early Cambrian is coincident with the εNd(t) variation in silicate detritus from Australia and NW Laurentia (Fig. 6A), suggesting enhanced denudation of old continental rock. The εNd(t) variation in shallow-marine carbonates in this study is consistent with long-term εNd(t) evolution of the Paleo-Pacific Ocean in the early Cambrian (Keto and Jacobsen, 1988), which is suggested as a global change in the supply of weathered continental materials to the ocean. In the early Cambrian, final assembly of Gondwana with widespread continental collision resulted in a high topographic landscape and a potentially low sea level (e.g., Li et al., 2013). Moreover, the early Cambrian was characterized by a greenhouse climate likely due to extensive subduction outgassing (McKenzie et al., 2016; Hearing et al., 2018). Hence, the decreased εNd(t) values, coincident with elevated $^{87}Sr/^{86}Sr$ ratios, from the carbonates in the Yanjiahe section are indicative of an intense continental weathering during the early Cambrian, consistent with previous studies (e.g., Maloof et al., 2010; Peters and Gaines, 2012).

5.3 Long-term evolution of εNd(t) in continental shelf seawater: more records from global shallow-marine sediments

Although the residence time of Nd in the ocean is very short (~ 600 yr, Johannesson and Burdige, 2007), temporal changes in εNd(t) values of epeiric seawater can potentially reflect gradual evolution of terrestrial inputs on the continental shelves, which may have been controlled by tectonic activity and climate change (e.g., Scher et al., 2011; Peters and Gaines, 2012). Due to the limited contribution from oceanic hydrothermal sources (Piepgras and Wasserburg, 1985; Goldstein and Jacobsen, 1987), the sedimentary εNd(t) record is more effective for directly tracking regionally terrestrial inputs and water sources, compared with $^{87}Sr/^{86}Sr$ or $^{187}Os/^{188}Os$ ratios. Shallow-marine carbonates in this study exhibit a long-term decreasing trend in εNd(t) values from the early Ediacaran to early Cambrian, superimposed by an abrupt negative excursion of εNd(t) values during the Shuram Excursion in the middle Ediacaran. Significantly negative εNd(t) values during the Shuram Excursion likely record incorporation of water-mass from the Laurentia. Whereas, the secular εNd(t) varying trend in shallow carbonates coincides with the evolution of εNd(t) in global terrestrial silicate detritus (Fig. 6A), suggesting a more dominant control of continental weathering materials on gradual change in εNd(t) values of continental shelf seawater over million-year timescale.

To better understand holistic εNd(t) variations of shallow seawater, εNd(t) record derived from shallow-marine carbonates in this study is combined with more εNd(t) records from phosphoric rocks (Yang et al., 1997; Felitsyn and Gubanov, 2002) in different regions from the Ediacaran to early Cambrian (Fig. 6B). εNd(t) values of continental shelf seawater derived from these shallow-marine sediments are further compared to εNd(t) record for Paleo-Pacific (Panthalassa) waters (shaded area in Fig. 6B, modified from Keto and Jacobsen, 1988).

Compilations of εNd(t) data from shallow-marine biotic and abiotic sediments show a relatively consistent and high εNd(t) composition (around –5) of shallow seawater from the Cryogenian to the middle Ediacaran which coincides with prolonged breakup of Rodinia. Appreciable drop in seawater εNd(t) values initially occurs in the middle Ediacaran and significantly low εNd(t) values (< –15) are observed in the early Cambrian (Fig. 6B). The initial decrease of seawater εNd(t) in the middle Ediacaran is coincident with the beginning of Gondwana assembly (Li et al., 2008, 2013). Further, the secular εNd(t) record from the early Ediacaran to early Cambrian is roughly consistent with the $^{87}Sr/^{86}Sr$ record in this study (Fig. 7) as well as long-term $^{87}Sr/^{86}Sr$ evolution during the late Neoproterozoic (e.g., Maloof et al., 2010), despite the exceedingly high $^{87}Sr/^{86}Sr$ in the Doushantuo cap dolostone which is likely deposited in a deglacial meltwater-seawater mixture (Wei et al., 2019). In conjunction with zircon O–Hf isotope record (e.g., Cawood et al., 2013; Spencer et al., 2014), Nd isotopic variations from the Ediacaran to early Cambrian (Fig. 7) are more likely associated with the final Rodinia breakup and subsequent Gondwana assembly. Significantly low εNd(t) values in the early Cambrian (< –15) are corresponding to peak and trough of zircon O isotope and Hf isotope values (Fig. 6, Cawood et al., 2013; Spencer et al., 2014), in response to the timing of extensive continental orogeny driven by final Gondwana assembly. In particular, the initiation of substantial changes in zircon O–Hf isotopes precedes the significant seawater εNd(t) decrease recorded in this study (Fig. 6B), indicating that the formation of mature continent-sourced rocks should be much earlier than weathering of these rocks. In conclusion, secular variation in shallow seawater εNd(t) directly results from changes in weathered materials exported to continental shelf area, driven by long-term tectonic activity.

5.4 Potential links between increased continental denudation and oceanic oxygenation in the terminal Precambrian

Several isotope systems, such as $^{87}Sr/^{86}Sr$, δ^7Li and $\delta^{44}Ca$, have been widely used to track the evolution of continental weathering (e.g., Blättler et al., 2011; Pogge von Strandmann et al., 2013; Chen et al., 2018). εNd(t) values of shallow-marine carbonates can provide a more direct clue for changes in the weathering of regional continental materials (old crust vs. juvenile rock) ultimately controlled by long-term tectonic activity, since differential weathering of silicate minerals in a single rock and submarine hydrothermal fluid have little effects on εNd(t) of continental shelf seawater (e.g., Goldstein and Jacobsen, 1987; Bayon et al., 2015). Although more data are needed from various continental margins for a global chemostratigraphic correlation, gradually decreasing εNd(t) values of shallow-marine carbonates as well as phosphatic rocks in this study support a gradually more extensive and intensive continental orogeny during the assembly of Gondwana from the middle Ediacaran to early Cambrian (Li et al., 2008, 2013; Zhao et al., 2018). Tectonic and magmatic processes are proposed closely linked with Precambrian atmospheric oxygenation (Campbell and Allen, 2008; Planavsky, 2018; Li et al., 2018). The net accumulation of atmospheric O_2 is generally determined by the fluxes of O_2 production and consumption. From the middle Ediacaran to early Cambrian, elevated topography following widespread mountain building related to the amalgamation of Gondwana would have enhanced continental denudation and nutrient export to continental marginal seawater which is supported by increased P contents in fine-grained marine siliciclastic rocks (Reinhard et al., 2017). Thus, O_2 release by marine primary production may have been promoted by this marine fertilization. In addition, the delivery of abundant detrital silicates to continental shelf margin can facilitate organic carbon burial via more rapid burial of marine clastic sediment, as observed in the modern Ganges-Brahmaputra basin (cf.

Galy et al., 2011, 2015), yielding a well positive correlation between organic carbon burial rate and sediment burial rate (Berner and Canfield, 1989). Moreover, a decline in volcanism in the period of intensive intracontinental collision within Gondwana leads to less release of reduced gases from the Earth's interior into the atmosphere (cf. Kump and Barley, 2007). Both enhanced organic carbon burial and decreased release of reduced gases result in less O_2 consumption at the Earth surface. In conclusion, the long-term overall increase in oxygen levels from the middle Ediacaran to early Cambrian is likely a result of secular accumulation of oxygen along with the prolonged assembly of the Gondwana and then extensive continental orogeny. Hence, enhanced continental denudation related to supercontinent assembly may have aroused the Earth-surface environment from a low O_2 steady state, which likely triggers the diversification and radiation of large, complex animals from the late Ediacaran to early Cambrian (Fig. 7).

6. Conclusions

Carbonates of the Ediacaran–Cambrian Jiulongwan–Gaojiaxi–Yanjiahe section, South China exhibit a gradually decreasing trend in εNd(t) values from around –4 to –8, which directly indicates a progressively intensifying export of weathered terrestrial materials to continental shelf seawater during the terminal Neoproterozoic and early Cambrian. Additionally, a significant and transient negative εNd(t) anomaly in the middle Ediacaran superimposed on the secular decreasing εNd(t) trend, which is indicative of an abrupt and rapid improvement of seawater transport from Laurentia to South China. Together with radiogenic Sr isotopes, the long-term evolution of εNd(t) values on the Yangtze continental margin from the Ediacaran to early Cambrian is considered to be dominantly controlled by extensive continental collision following the assembly of Gondwana.

The rise of oxygen level in Earth-surface environment during this key transition is proposed to be linked with enhanced continental weathering, driven by continued continental orogenic processes.

Acknowledgements

We thank Liang Li and Weiwei Xue for assistance with the lab work. We deeply appreciate Prof. Thomas Algeo and Prof. Chao Li for editing this paper, Dr. Huan Cui and an anonymous reviewer for their constructive comments. This study was funded by the Strategic Priority Research Program (B) of the Chinese Academy of Sciences (CAS) (XDB26000000) and the National Natural Science Foundation of China (NSFC) program (41872002, 41661134048). Guang-Yi Wei is also funded by the program A for Outstanding PhD. Candidate of Nanjing University (No. 201802A020).

References

Abbott, A. N., Haley, B. A. and McManus, J., 2016. The impact of sedimentary coatings on the diagenetic Nd flux. Earth and Planetary Science Letters 449, 217-227.

Albarède, F., Goldstein, S. L., 1992. World map of Nd isotopes in sea-floor ferromanganese deposit. Geology 20, 761-763.

Allègre, C. J., 2008. Isotope Geology. Cambridge University Press. (534 pp).

Bailey, T. R., McArthur, J. M., Prince, H. and Thirlwall, M. F., 2000. Dissolution methods for strontium isotope stratigraphy: whole rock analysis. Chemical Geology 167, 313-319.

Bau, M. and Alexander, B., 2006. Preservation of primary REE patterns without Ce anomaly during dolomitization of Mid-Paleoproterozoic limestone and the potential re-establishment of marine anoxia immediately after the "Great Oxidation Event". South African Journal of Geology 109, 81-86.

Bayon, G., Toucanne, S., Skonieczny, C., André, L., Bermell, S., Cheron, S., Dennielou, B., Etoubleau, J., Freslon, N., Gauchery, T., Germain, Y., Jorry, S. J., Ménot, G., Monin, L., Ponzevera, E., Rouget, M. L., Tachikawa, K. and Barrat, J. A., 2015. Rare earth elements and neodymium isotopes in world river sediments revisited. Geochimica et Cosmochimica Acta 170, 17-38.

Berglund, M., Wieser, M.E., 2011. Isotopic compositions of the elements 2009 (IUPAC Technical Report). Pure & Applied Chemistry 85, 1047-1078.

Berner, R. and Canfield, D. E., 1989. A new model for atmospheric oxygen over Phanerozoic time. American Journal of Science 289, 333-361.

Blättler, C. L., Jenkyns, H. C., Reynard, L. M. and Henderson, G. M., 2011. Significant increases in global weathering during Oceanic Anoxic Events 1a and 2 indicated by calcium isotopes. Earth and Planetary Science Letters 309, 77-88.

Blum, J. D. and Erel, Y., 1995. A silicate weathering mechanism linking increases in marine $^{87}Sr/^{86}Sr$ with global glaciation. Nature 373, 415-418.

Campbell, I. H. and Allen, C. M., 2008. Formation of supercontinents linked to increases in atmospheric oxygen. Nature Geoscience 1, 554-558.

Canfield, D. E., Poulton, S. W. and Narbonne, G. M., 2007. Late-Neoproterozoic deep-ocean oxygenation and the rise of animal life. Science 315, 92-95.

Cawood, P. A., Hawkesworth, C. J. and Dhuime, B., 2013. The continental record and the generation of continental crust. Geological Society of America Bulletin 125, 14-32.

Chen, P., 1984. Discovery of Lower Cambrian small shelly fossils from Jijiapo Yichang, west Hubei and its significance. Professional Papers of Stratigraphy and Palaeontology 13, 49-66.

Chen, J., Montañez, I. P., Qi, Y., Shen, S. and Wang, X., 2018. Strontium and carbon isotopic evidence for decoupling of pCO2 from continental weathering at the apex of the late Paleozoic glaciation. Geology 46, 395-398.

Chen, X., Romaniello, S. J., Herrmann, A. D., Hardisty, D., Gill, B. C. and Anbar, A. D., 2018. Diagenetic effects on uranium isotope fractionation in carbonate sediments from the Bahamas. Geochimica et Cosmochimica Acta 237, 294-311.

Chen, Z., Zhou, C., Xiao, S., Wang, W., Guan, C., Hua, H., Yuan, X., 2014. New Ediacara fossils preserved in marine limestone and their ecological implications. Scientific Reports 4, 4180.

Condon, D., Zhu M., Bowring, S., Wang W., Yang, A., Jin, Y., 2005. U-Pb Ages from the Neoproterozoic Doushantuo Formation, China. Science 308, 95-98.

Cox, G. M., Halverson, G. P., Stevenson, R. K., Vokaty, M., Poirier, A., Kunzmann, M., Li, Z.-X., Denyszyn, S. W., Strauss, J. V. and Macdonald, F. A., 2016. Continental flood basalt weathering as a trigger for Neoproterozoic Snowball Earth. Earth and Planetary Science Letters 446, 89-99.

Dera, G., Prunier, J., Smith, P. L., Haggart, J. W., Popov, E., Guzhov, A., Rogov, M., Delsate, D., Thies, D., Cuny, G., Pucéat, E., Charbonnier, G. and Bayon, G., 2015. Nd isotope constraints on ocean circulation, paleoclimate, and continental drainage during the Jurassic breakup of Pangea. Gondwana Research 27, 1599-1615.

Dopieralska, J., Belka, Z. and Walczak, A., 2016. Nd isotope composition of conodonts: An accurate proxy of sea-level fluctuations. Gondwana Research 34, 284-295.

Du, J., Haley, B. A. and Mix, A. C., 2016. Neodymium isotopes in authigenic phases, bottom waters and detrital sediments in the Gulf of Alaska and their implications for paleo-circulation reconstruction. Geochimica et Cosmochimica Acta 193, 14-35.

Fanton, K. C., Holmden, C., Nowlan, G. S., Haidl, F. M., 2002. $^{143}Nd/^{144}Nd$ and Sm/Nd stratigraphy of Upper Ordovician epritic sea carbonates. Geochemica et Cosmochimica Acta 66, 241-255.

Felitsyn, S. B. and Gubanov, A. P., 2002. Nd isotope composition of early Cambrian discrete basins. Geological Magazine 139, 159-169.

Frank, M., 2002. Radiogenic isotopes: Tracers of past ocean circulation and erosional input. Reviews of Geophysics 40, 1.

Galy, V. and Eglinton, T., 2011. Protracted storage of biospheric carbon in the Ganges–Brahmaputra basin. Nature Geoscience 4, 843-847.

Galy, V., Peucker-Ehrenbrink, B. and Eglinton, T., 2015. Global carbon export from the terrestrial biosphere controlled by erosion. Nature 521, 204-207.

Gernon, T. M., Hincks, T. K., Tyrrell, T., Rohling, E. J. and Palmer, M. R., 2016. Snowball Earth ocean chemistry driven by extensive ridge volcanism during Rodinia breakup. Nature Geoscience 9, 242-248.

Goldstein, S. L. and Hemming, S. R., 2014. Long-lived Isotopic Tracers in Oceanography, Paleoceanography, and Ice-sheet Dynamics. Treatise on Geochemistry, 2nd Edition, 453-483.

Goldstein, S. J. and Jacobsen, S. B., 1987. The Nd and Sr isotopic systematics of river-water dissolved material: Implications for the sources of Nd and Sr in seawater. Chemical Geology: Isotope Geoscience section 66, 245-272.

Gong, Z., Kodama, K. P. and Li, Y.-X., 2017. Rock magnetic cyclostratigraphy of the Doushantuo Formation, South China and its implications for the duration of the Shuram carbon isotope excursion. Precambrian Research 289, 62-74.

Grandjean, P., Cappetta, H. and Albarède, F., 1988. The REE and εNd(t) of 40-70 Ma old fish debris from the west-African platform. Geophysical Research Letters 15, 389-392.

Grotzinger, J. P., Fike, D. A. and Fischer, W., 2011. Enigmatic origin of the largest-known carbon isotope excursion in Earth's history. Nature Geoscience 4, 285-292.

Hearing, T. W., Harvey, T. H. P., Williams, M., Leng, M. J., Lamb, A. L., Wilby, P. R., Gabbott, S. E., Pohl, A., Donnadieu, Y., 2018. An early Cambrian greenhouse climate. Science Advances 4, eaar5690.

Higgins, J. A., Blättler, C. L., Lundstrom, E. A., Santiago-Ramos, D. P., Akhtar, A. A., Crüger Ahm, A. S., Bialik, O., Holmden, C., Bradbury, H., Murray, S. T. and Swart, P. K., 2018. Mineralogy, early marine diagenesis, and the chemistry of shallow-water carbonate sediments. Geochimica et Cosmochimica Acta 220, 512-534.

Hirahara, Y., Chang, Q., Miyazaki, T., Takahashi, T. and Kimura, J.-I., 2012. Improved Nd chemical separation technique for $^{143}Nd/^{144}Nd$ analysis in geological samples using packed Ln resin columns. JAMSTEC Report of Research and Development 15, 27-33.

Hoffman, P. F., Abbot, D. S., Ashkenazy, Y., Benn, D. I., Brocks, J. J., Cohen, P. A., Cox, G. M., Creveling, J. R., Donnadieu, Y., Erwin, D. H., Fairchild, I. J., Ferreira, D., Goodman, J. C., Halverson, G. P., Jansen, M. F., Le Hir, G., Love, G. D., Macdonald, F. A., Maloof, A. C., Partin, C. A., Ramstein, G., Rose, B. E. J., Rose, C. V., Sadler, P. M., Tziperman, E., Voigt, A. and Warren, S. G., 2017. Snowball Earth climate dynamics and Cryogenian geology-geobiology. Science Advances 3, e1600983.

Hoffman, P. F. and Li, Z.-X., 2009. A palaeogeographic context for Neoproterozoic glaciation. Palaeogeography, Palaeoclimatology, Palaeoecology 277, 158-172.

Holmden, C., Creaser, R. A., Muehlenbachs, K., Leslie, S. A. and Bergstrom, S. M., 1998. Isotopic evidence for geochemical decoupling between ancient epeiric seas and bordering oceans: Implications for secular curves. Geology 26, 567-570.

Holmden, C., Mitchell, C. E., LaPorte, D. F., Patterson, W. P., Melchin, M. J. and Finney, S. C., 2013. Nd isotope records of late Ordovician sea-level change—Implications for glaciation frequency and global stratigraphic correlation. Palaeogeography, Palaeoclimatology, Palaeoecology 386, 131-144.

Hu, R., Wang, W., Li, S.-Q., Yang, Y.-Z. and Chen, F., 2016. Sedimentary Environment of Ediacaran Sequences of South China: Trace Element and Sr-Nd Isotope Constraints. The Journal of Geology 124, 769-789.

Jacobsen, S. B. and Wasserburg, G. J., 1980. Sm-Nd isotopic evolution of chondrites. Earth and Planetary Science Letters 50, 139-155.

Jang, K., Huh, Y. and Han, Y., 2018. Diagenetic overprint on authigenic Nd isotope records: A case study of the Bering Slope. Earth and Planetary Science Letters 498, 247-256.

Jiang, G., Shi, X., Zhang, S., Wang, Y. and Xiao, S., 2011. Stratigraphy and paleogeography of the Ediacaran Doushantuo Formation (ca. 635–551Ma) in South China. Gondwana Research 19, 831-849.

Jiang, G., Wang, X., Shi, X., Xiao, S., Zhang, S. and Dong, J., 2012. The origin of decoupled carbonate and organic carbon isotope signatures in the early Cambrian (ca. 542–520Ma) Yangtze platform. Earth and Planetary Science Letters 317-318, 96-110.

Johannesson, K. H. and Burdige, D. J., 2007. Balancing the global oceanic neodymium budget: Evaluating the role of groundwater. Earth and Planetary Science Letters 253, 129-142.

Keto, L. S. and Jacobsen, S. B., 1988. Nd isotopic variations of Phanerozoic paleoceans. Earth and Planetary Science Letters 90, 395-410.

Knoll, A. H., Nowak, M. A., 2017. The timetable of evolution. Science Advances 3, e1603076.

Kump, L. R. and Barley, M. E., 2007. Increased subaerial volcanism and the rise of atmospheric oxygen 2.5 billion years ago. Nature 448, 1033-1036.

Lacan, F. and Jeandel, C., 2004. Neodymium isotopic composition and rare earth element concentrations in the deep and intermediate Nordic Seas: Constraints on the Iceland Scotland Overflow Water signature. Geochemistry, Geophysics, Geosystems 5, Q11006.

Lacan, F., Tachikawa, K. and Jeandel, C., 2012. Neodymium isotopic composition of the oceans: A compilation of seawater data. Chemical Geology 300-301, 177-184.

Li, C., Cheng, M., Zhu, M. and Lyons, T. W., 2018. Heterogeneous and dynamic marine shelf oxygenation and coupled early animal evolution. Emerging Topics in Life Sciences 2, 279-288.

Li, D., Shields-Zhou, G. A., Ling, H.-F. and Thirlwall, M., 2011. Dissolution methods for strontium isotope stratigraphy: Guidelines for the use of bulk carbonate and phosphorite rocks. Chemical Geology 290, 133-144.

Li, G., Chen, J., Ji, J., Liu, L., Yang, J. and Sheng, X., 2007. Global cooling forced increase in marine strontium isotopic ratios: Importance of mica weathering and a kinetic approach. Earth and Planetary Science Letters 254, 303-312.

Li, Z. X., Bogdanova, S. V., Collins, A. S., Davidson, A., De Waele, B., Ernst, R. E., Fitzsimons, I. C. W., Fuck, R. A., Gladkochub, D. P., Jacobs, J., Karlstrom, K. E., Lu, S., Natapov, L. M., Pease, V., Pisarevsky, S. A., Thrane, K. and Vernikovsky, V., 2008. Assembly, configuration, and break-up history of Rodinia: A synthesis. Precambrian Research 160, 179-210.

Li, Z.-X., Evans, D. A. D. and Halverson, G. P., 2013. Neoproterozoic glaciations in a revised global palaeogeography from the breakup of Rodinia to the assembly of Gondwanaland. Sedimentary Geology 294, 219-232.

Ling, H.-F., Chen, X., Li, D., Wang, D., Shields-Zhou, G. A. and Zhu, M., 2013. Cerium anomaly variations in Ediacaran–earliest Cambrian carbonates from the Yangtze Gorges area, South China: Implications for oxygenation of coeval shallow seawater. Precambrian Research 225, 110-127.

Liu, X.-M., Hardisty, D. S., Lyons, T. W. and Swart, P. K., 2019. Evaluating the fidelity of the cerium paleoredox tracer during variable carbonate diagenesis on the Great Bahamas Bank. Geochimica et Cosmochimica Acta 248, 25-42.

Lu, M., Zhu, M., Zhang, J., Shields-Zhou, G., Li, G., Zhao, F., Zhao, X. and Zhao, M., 2013. The DOUNCE event at the top of the Ediacaran Doushantuo Formation, South China: Broad stratigraphic occurrence and non-diagenetic origin. Precambrian Research 225, 86-109.

Lugmair, G.W., Marti, K., 1978. Lunar initial 143 Nd/ 144 Nd: Differential evolution of the lunar crust and mantle. Earth & Planetary Science Letters 39, 349-357.

Lyons, T. W., Reinhard, C. T. and Planavsky, N. J., 2014. The rise of oxygen in Earth's early ocean and atmosphere. Nature 506, 307-315.

Maloof, A. C., Porter, S. M., Moore, J. L., Dudas, F. O., Bowring, S. A., Higgins, J. A., Fike, D. A. and Eddy, M. P., 2010. The earliest Cambrian record of animals and ocean geochemical change. Geological Society of America Bulletin 122, 1731-1774.

Mckenzie N. R., H. B. K., Loomis S. E., Stockli D. F., Planavsky N. J., Lee C. T., 2016. Continental arc volcanism as the principal driver of icehouse-greenhouse variability. Science 352, 444-447.

Minguez, D. and Kodama, K. P., 2017. Rock magnetic chronostratigraphy of the Shuram carbon isotope excursion: Wonoka Formation, Australia. Geology 45, 567-570.

McFadden, K. A., Huang, J., Chu, X., Jiang, G., Kaufman, A. J., Zhou, C., Yuan, X. and Xiao, S., 2008. Pulsed oxidation and biological evolution in the Ediacaran Doushantuo Formation. Proc Natl Acad Sci USA 105, 3197-3202.

Meija, J., Coplen, T.B., Berglund, M., Brand, W.A., Prohaska, T., 2016. Atomic weights of the elements 2013 (IUPAC Technical Report). Pure and Applied Chemistry 88, 265-291.

Narbonne, G. M., Xiao, S. and Shields, G. A., 2012. The Ediacaran Period. In *The Geologic Time Scale*. Elsevier B. V., 413-435.

Nothdurft, L. D., Webb, G. E. and Kamber, B. S., 2004. Rare earth element geochemistry of Late Devonian reefal carbonates, Canning Basin, Western Australia: confirmation of a seawater REE proxy in ancient limestones. Geochimica et Cosmochimica Acta 68, 263-283.

Och, L. M. and Shields-Zhou, G. A., 2012. The Neoproterozoic oxygenation event: Environmental perturbations and biogeochemical cycling. Earth-Science Reviews 110, 26-57.

Peters, S. E. and Gaines, R. R., 2012. Formation of the 'Great Unconformity' as a trigger for the Cambrian explosion. Nature 484, 363-366.

Piepgras, D. J. and Wasserburg, G. J., 1982. Isotopic composition of neodymium in waters from the drake passage. Science 217, 207-214.

Piepgras, D. J. and Wasserburg, G. J., 1985. Strontium and neodymium isotopes in hot springs on the East Pacific Rise and Guaymas Basin. Earth and Planetary Science Letters 72, 341-356.

Planavsky, N., 2018. From orogenies to oxygen. Nature Geoscience 11, 9-10.

Pogge von Strandmann, P. A. E., Jenkyns, H. C. and Woodfine, R. G., 2013. Lithium isotope evidence for enhanced weathering during Oceanic Anoxic Event 2. Nature Geoscience 6, 668-672.

Prestrud Anderson, S., Drever, J. I. and Humphrey, N. F., 1997. Chemical weathering in glacial environment. Geology 25, 399-402.

Pu, J. P., Bowring, S. A., Ramezani, J., Myrow, P., Raub, T. D., Landing, E., Mills, A., Hodgin, E. and Macdonald, F. A., 2016. Dodging snowballs: Geochronology of the Gaskiers glaciation and the first appearance of the Ediacaran biota. Geology 44, 955-958.

Reinhard, C. T., Planavsky, N. J., Gill, B. C., Ozaki, K., Robbins, L. J., Lyons, T. W., Fischer, W. W., Wang, C., Cole, D. B. and Konhauser, K. O., 2017. Evolution of the global phosphorus cycle. Nature 541, 386-389.

Sahoo, S. K., Planavsky, N. J., Jiang, G., Kendall, B., Owens, J. D., Wang, X., Shi, X., Anbar, A. D. and Lyons, T. W., 2016. Oceanic oxygenation events in the anoxic Ediacaran ocean. Geobiology 14, 457-468.

Scher, H. D., Bohaty, S. M., Zachos, J. C. and Delaney, M. L., 2011. Two-stepping into the icehouse: East Antarctic weathering during progressive ice-sheet expansion at the Eocene–Oligocene transition. Geology 39, 383-386.

Shields, G. A., 2005. Neoproterozoic cap carbonates: a critical appraisal of existing models and the plumeworld hypothesis. Terra Nova 17, 299-310.

Spencer, C. J., Cawood, P. A., Hawkesworth, C. J., Raub, T. D., Prave, A. R. and Roberts, N. M. W., 2014. Proterozoic onset of crustal reworking and collisional tectonics: Reappraisal of the zircon oxygen isotope record. Geology 42, 451-454.

Sperling, E. A., Frieder, C. A., Raman, A. V., Girguis, P. R., Levin, L. A. and Knoll, A. H., 2013. Oxygen, ecology, and the Cambrian radiation of animals. Proc Natl Acad Sci U S A 110, 13446-13451.

Stewart, J. A., Gutjahr, M., Pearce, F., Swart, P. K. and Foster, G. L., 2015. Boron during meteoric diagenesis and its potential implications for Marinoan snowball Earth δ^{11}B-pH excursions. Geology 43, 627-630.

Tachikawa, K., Arsouze, T., Bayon, G., Bory, A., Colin, C., Dutay, J.-C., Frank, N., Giraud, X., Gourlan, A. T., Jeandel, C., Lacan, F., Meynadier, L., Montagna, P., Piotrowski, A. M., Plancherel, Y., Pucéat, E., Roy-Barman, M. and Waelbroeck, C., 2017. The large-scale evolution of neodymium isotopic composition in the global modern and Holocene ocean revealed from seawater and archive data. Chemical Geology 457, 131-148.

Taylor, S. and McLennan, S., 1985. The Continental Crust: Its Composition and Evolution. Blackwell Scientific Publications. (312 pp.)

Tissot, F. L. H., Chen, C., Go, B. M., Naziemiec, M., Healy, G., Bekker, A., Swart, P. K. and Dauphas, N., 2018. Controls of eustasy and diagenesis on the ^{238}U/^{235}U of carbonates and evolution of the seawater (^{234}U/^{238}U) during the last 1.4 Myr. Geochimica et Cosmochimica Acta 242, 233-265.

Wang, Z., Wang, J., Suess, E., Wang, G., Chen, C. and Xiao, S., 2017. Silicified glendonites in the Ediacaran Doushantuo Formation (South China) and their potential paleoclimatic implications. Geology 45, 115-118.

Webb, G. E. and Kamber, B. S., 2000. Rare earth elements in Holocene reefal microbialites: A new shallow seawater proxy. Geochemica et Cosmochimica Acta 64, 1557-1565.

Webb, G. E., Nothdurft, L. D., Kamber, B. S., Kloprogge, J. T. and Zhao, J.-X., 2009. Rare earth element geochemistry of scleractinian coral skeleton during meteoric diagenesis: a sequence through neomorphism of aragonite to calcite. Sedimentology 56, 1433-1463.

Wei, G.-Y., Hood, A. v.S., Chen, X., Li, D., Wei, W., Wen, B., Gong, Z., Yang, T., Zhang, Z.-F. and Ling, H.-F., 2019. Ca and Sr isotope constraints on the formation of the Marinoan cap dolostones. Earth and Planetary Science Letters 511, 202-212.

Wei, G.-Y., Planavsky, N. J., Tarhan, L. G., Chen, X., Wei, W., Li, D. and Ling, H.-F., 2018. Marine redox fluctuation as a potential trigger for the Cambrian explosion. Geology 46, 587-590.

Wood, R., Liu, A.G., Bowyer, F., Wilby, P.R., Dunn, F.S., Kenchington, C.G., Cuthill, J.F.H., Mitchell, E.G., Penny, A., 2019. Integrated records of environmental change and evolution challenge the Cambrian Explosion. Nature Ecology & Evolution.

Wood, R. A., Poulton, S. W., Prave, A. R., Hoffmann, K. H., Clarkson, M. O., Guilbaud, R., Lyne, J. W., Tostevin, R., Bowyer, F., Penny, A. M., Curtis, A. and Kasemann, S. A., 2015. Dynamic redox conditions control late Ediacaran metazoan ecosystems in the Nama Group, Namibia. Precambrian Research 261, 252-271.

Xu, Y., Cawood, P. A., Du, Y., Hu, L., Yu, W., Zhu, Y. and Li, W., 2013. Linking south China to northern Australia and India on the margin of Gondwana: Constraints from detrital zircon U-Pb and Hf isotopes in Cambrian strata. Tectonics 32, 1547-1558.

Yang, J., Tao, X., Xue, Y., 1997. Nd isotope variations of Chinese seawater during Neoproterozoic through Cambrian. Chemical Geology 135, 127-137.

Zhang, F., Xiao, S., Kendall, B., Romaniello, S. J., Cui, H., Meyer, M., Gilleaudeau, G. J., Kaufman, A. J. and Anbar, A. D., 2018. Extensive marine anoxia during the terminal Ediacaran Period. Science Advances 4, eaan8983.

Zhao, G., Wang, Y., Huang, B., Dong, Y., Li, S., Zhang, G. and Yu, S., 2018. Geological reconstructions of the East Asian blocks: From the breakup of Rodinia to the assembly of Pangea. Earth-Science Reviews 186, 262-286.

Zhao, M.-Y. and Zheng, Y.-F., 2014. Marine carbonate records of terrigenous input into Paleotethyan seawater: Geochemical constraints from Carboniferous limestones. Geochemica et Cosmochimica Acta 141, 508-531.

Zhao, M.-Y. and Zheng, Y.-F., 2017. A geochemical framework for retrieving the linked depositional and diagenetic histories of marine carbonates. Earth and Planetary Science Letters 460, 213-221.

Zheng, X.-Y., Jenkyns, H. C., Gale, A. S., Ward, D. J. and Henderson, G. M., 2013. Changing ocean circulation and hydrothermal inputs during Ocean Anoxic Event 2 (Cenomanian–Turonian): Evidence from Nd-isotopes in the European shelf sea. Earth and Planetary Science Letters 375, 338-348.

Zheng, X.-Y., Jenkyns, H. C., Gale, A. S., Ward, D. J. and Henderson, G. M., 2016. A climatic control on reorganization of ocean circulation during the mid-Cenomanian event and Cenomanian-Turonian oceanic anoxic event (OAE 2): Nd isotope evidence. Geology 44, 151-154.

Figure captions

Figure 1. (A) Paleogeographic map of the Yangtze Block, South China (modified after Jiang et al., 2011). The studied area is at the Yangtze Gorges area, representing a sedimentary environment of intrashelf sedimentary basin. (B) Geological map of the Yangtze Gorges area, South China. Samples in this study are collected from 1) the Jiulongwan section; 2) the Gaojiaxi section; 3) the Yanjiahe section.

Figure 2. The profiles of (A) carbon, (B) radiogenic neodymium and (D) radiogenic strontium isotopic compositions as well as (C) neodymium concentrations from the carbonates in Jiulongwan-Gaojiaxi-Yanjiahe section, Yangtze Gorges area, South China. $[Nd]_{bulk}$ and $\varepsilon Nd(t)(t)_{bulk}$ represent the pristine data for Nd concentration and Nd isotope without correction of detrital component. $\delta^{13}C$ and $^{87}Sr/^{86}Sr$ data are referred from Ling et al. (2013); Wei et al. (2019) and this study.

Figure 3. Cross-plots of (A) $[Nd]_{bulk}$ vs. [Al], (B) $\varepsilon Nd(t)_{bulk}$ vs. [Al], (C) $[Nd]_{bulk}$ vs. [Th], (D) $\varepsilon Nd(t)_{bulk}$ vs. [Th] in bulk carbonates from Jiulongwan-Gaojiaxi-Yanjiahe section, Yangtze Gorges area, South China.

Figure 4. Calculated results of Nd concentration and εNd(t) value of pure carbonate component (presented as $[Nd]_{carb}$ and $\varepsilon Nd(t)_{carb}$, respectively), compared with bulk carbonate $[Nd]_{bulk}$ and $\varepsilon Nd(t)_{bulk}$ in this study.

Figure 5. Cross-plots of (A) $\varepsilon Nd(t)_{bulk}$ vs. $[Nd]_{bulk}$, (B) $\varepsilon Nd(t)_{carb}$ vs. $[Nd]_{carb}$, (C) $[Nd]_{carb}$ vs. Mg/Ca and (D) $\varepsilon Nd(t)_{carb}$ vs. Mg/Ca for carbonate samples in this study.

Figure 6. (A) $\varepsilon Nd(t)_{carb}$ variations in shallow carbonates from the early Ediacaran to early Cambrian in this study (filled circles), compared with secular evolution of εNd(t) in continental clasitc sediments from NW Laurentia, Australia, South China and Svalbard (data

from Cox et al., 2016) (squares). Nd isotopic compositions in marine carbonates, which are considered to record regionally shallow seawater signatures in this study, are overall higher than those in continental detritus, indicating that more dissolved mafic components from weathering of continental crust, than those from felsic components, are exported to shallow seawater. This observation also suggests a more congruent weathering for mafic rock than felsic rock. (B) Compilations of potential seawater εNd(t) records derived from shallow carbonates (this study), sedimentary phosphorites (Yang et al., 1997) and phosphatic Small Shelly Fossils (Felitsyn and Gubanov, 2002). Shaded area is the estimated εNd(t) range for paleo-pacific (Panthalassa) seawater (Keto and Jacobsen, 1988). The dashed curves are zircon Hf and O isotope records, modified from Cawood et al. (2013) and Spencer et al. (2014).

Figure 7. Co-varying $\varepsilon Nd(t)_{carb}$ and $^{87}Sr/^{86}Sr$ of shallow carbonates from the early Ediacaran to early Cambrian in this study in step with temporal occurrence ranges for key events of biological evolution (modified after Wood et al., 2019). The black solid curves are results of LOWESS smooth fitting for both $^{87}Sr/^{86}Sr$ and $\varepsilon Nd(t)_{carb}$ data in this study. The dashed curves are analytical errors for the LOWESS fitting (2 SD).

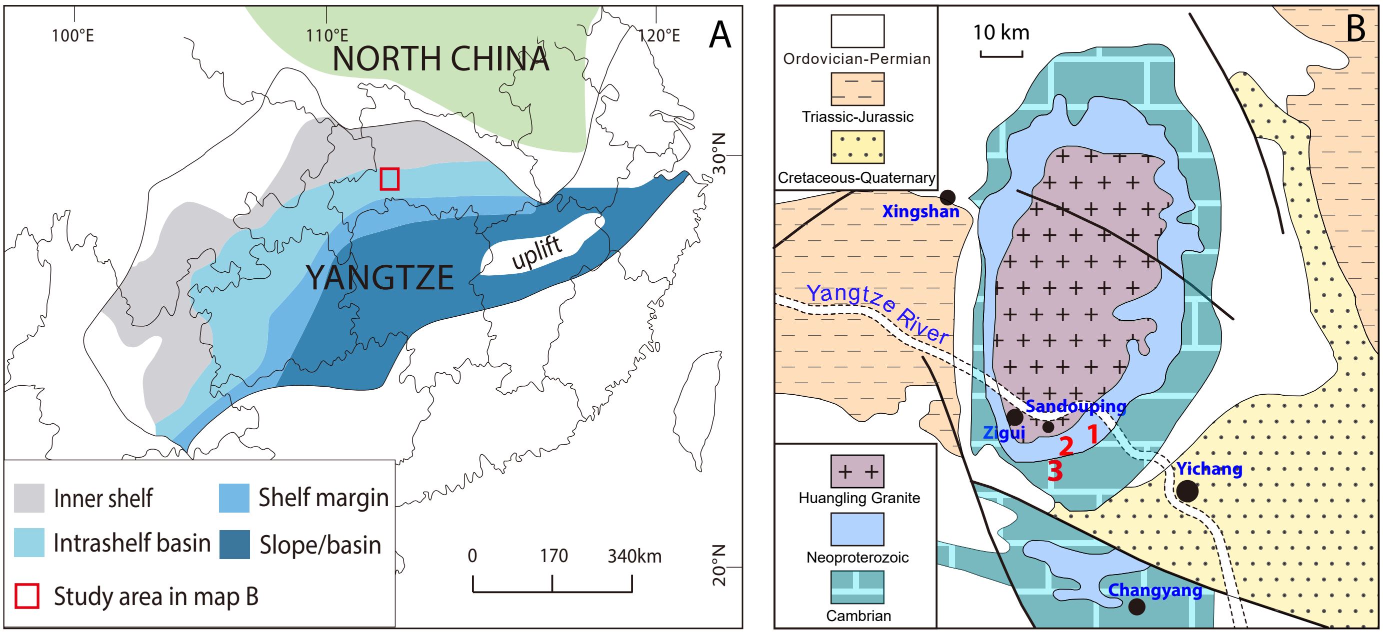

100°E
110°E
120°E
A
NORTH CHINA
30°N
YANGTZE
uplift
20°N
Inner shelf
Shelf margin
Intrashelf basin
Slope/basin
Study area in map B
0
170
340km
B
10 km
Ordovician-Permian
Triassic-Jurassic
Cretaceous-Quaternary
Xingshan
Yangtze River
Sandouping
Zigui
1
2
3
Yichang
Changyang
Huangling Granite
Neoproterozoic
Cambrian

Figure 1

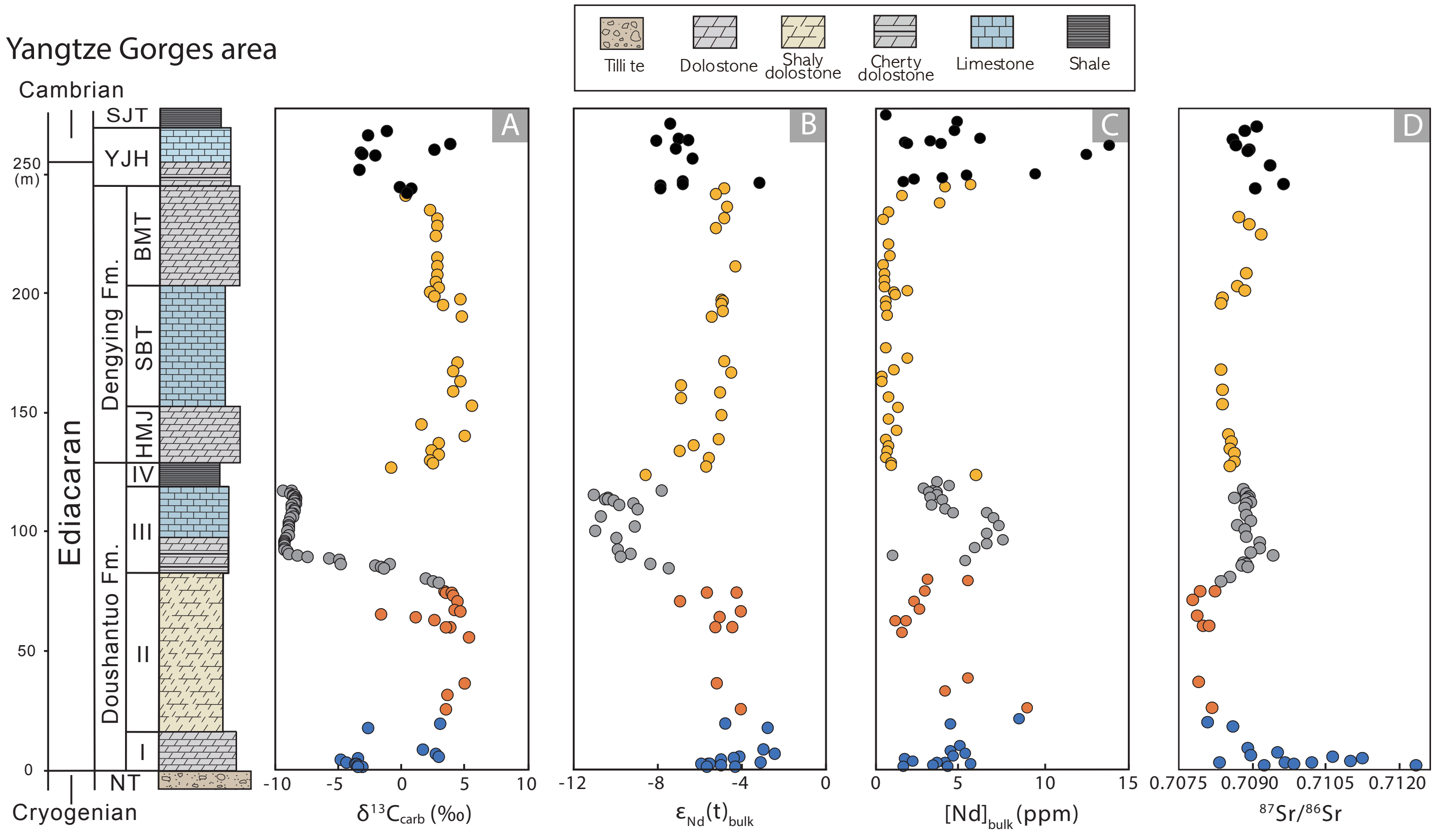

Yangtze Gorges area
Tilli te
Dolostone
Shaly dolostone
Cherty dolostone
Limestone
Shale
Cambrian
Cryogenian
Ediacaran
Dengying Fm.
Doushantuo Fm.
SJT
YJH
BMT
SBT
HMJ
IV
III
II
I
NT
250 (m)
200
150
100
50
0
A
B
C
D
-10
-5
0
5
10
-12
-8
-4
0
15
0.7075
0.7090
0.7105
0.7120
$\delta^{13}C_{carb}$ (‰)
$\varepsilon_{Nd}(t)_{bulk}$
$[Nd]_{bulk}$ (ppm)
$^{87}Sr/^{86}Sr$

Figure 2

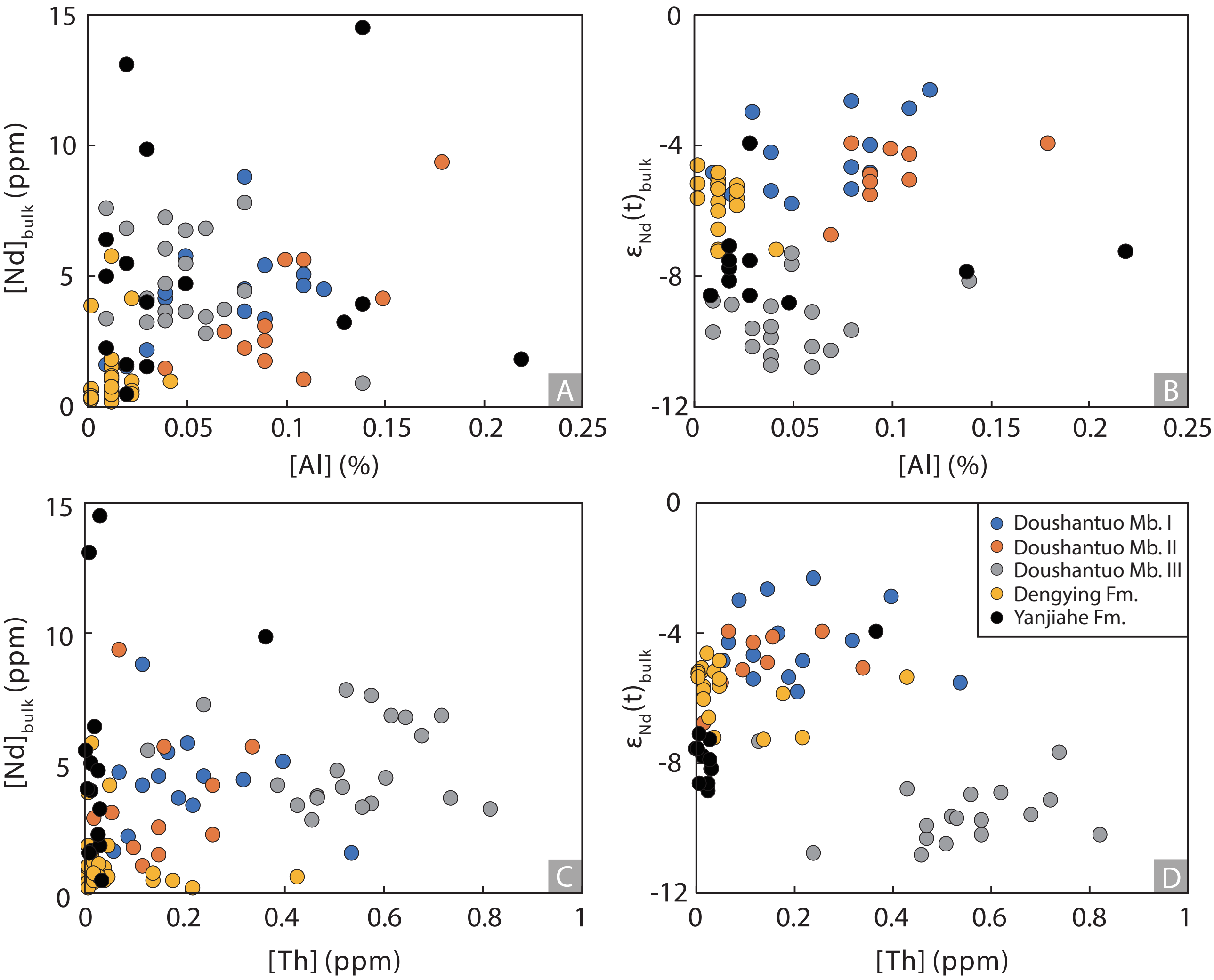

15
10
5
0
[Nd]bulk (ppm)
0
0.05
0.1
0.15
0.2
0.25
[Al] (%)
A
0
-4
-8
-12
εNd(t)bulk
B
C
[Th] (ppm)
0.2
0.4
0.6
0.8
1
D
Doushantuo Mb. I
Doushantuo Mb. II
Doushantuo Mb. III
Dengying Fm.
Yanjiahe Fm.

Figure 3

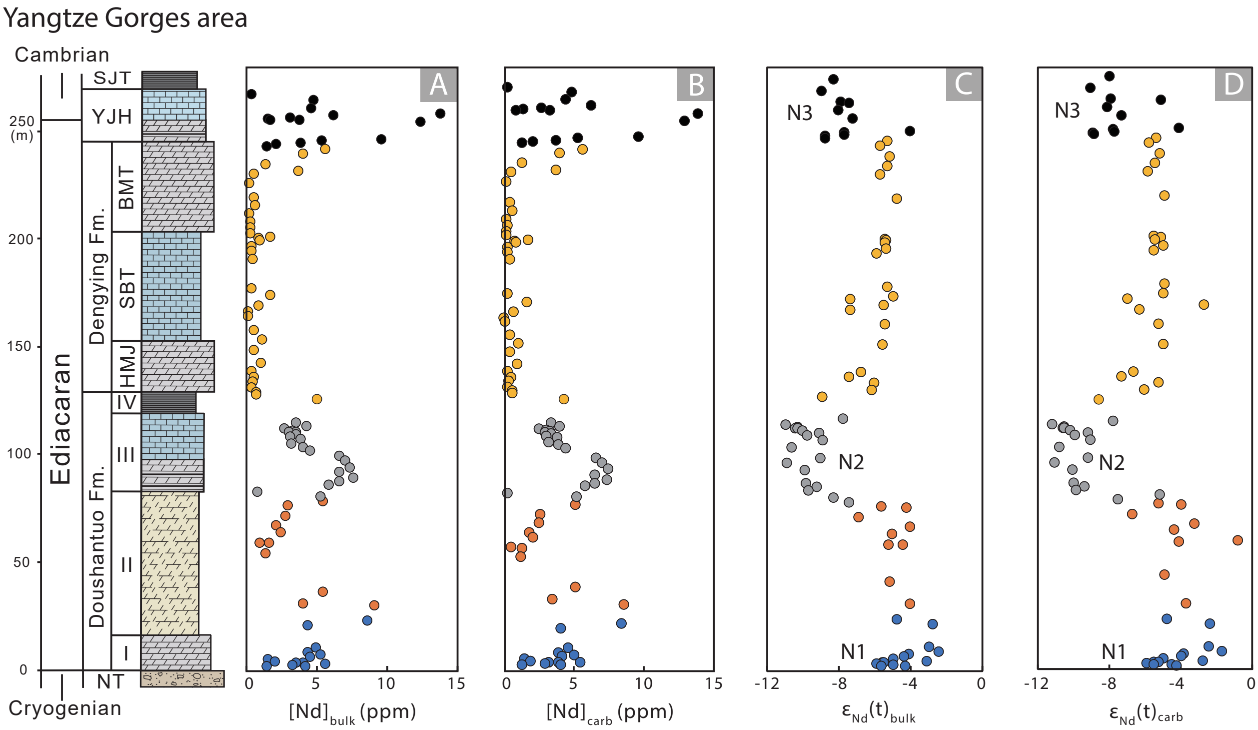
Yangtze Gorges area
Cambrian
SJT
YJH
BMT
SBT
HMJ
Dengying Fm.
IV
III
II
I
Doushantuo Fm.
Ediacaran
NT
Cryogenian
250 (m)
200
150
100
50
0
A
B
C
D
N3
N2
N1
[Nd]bulk (ppm)
[Nd]carb (ppm)
εNd(t)bulk
εNd(t)carb

Figure 4

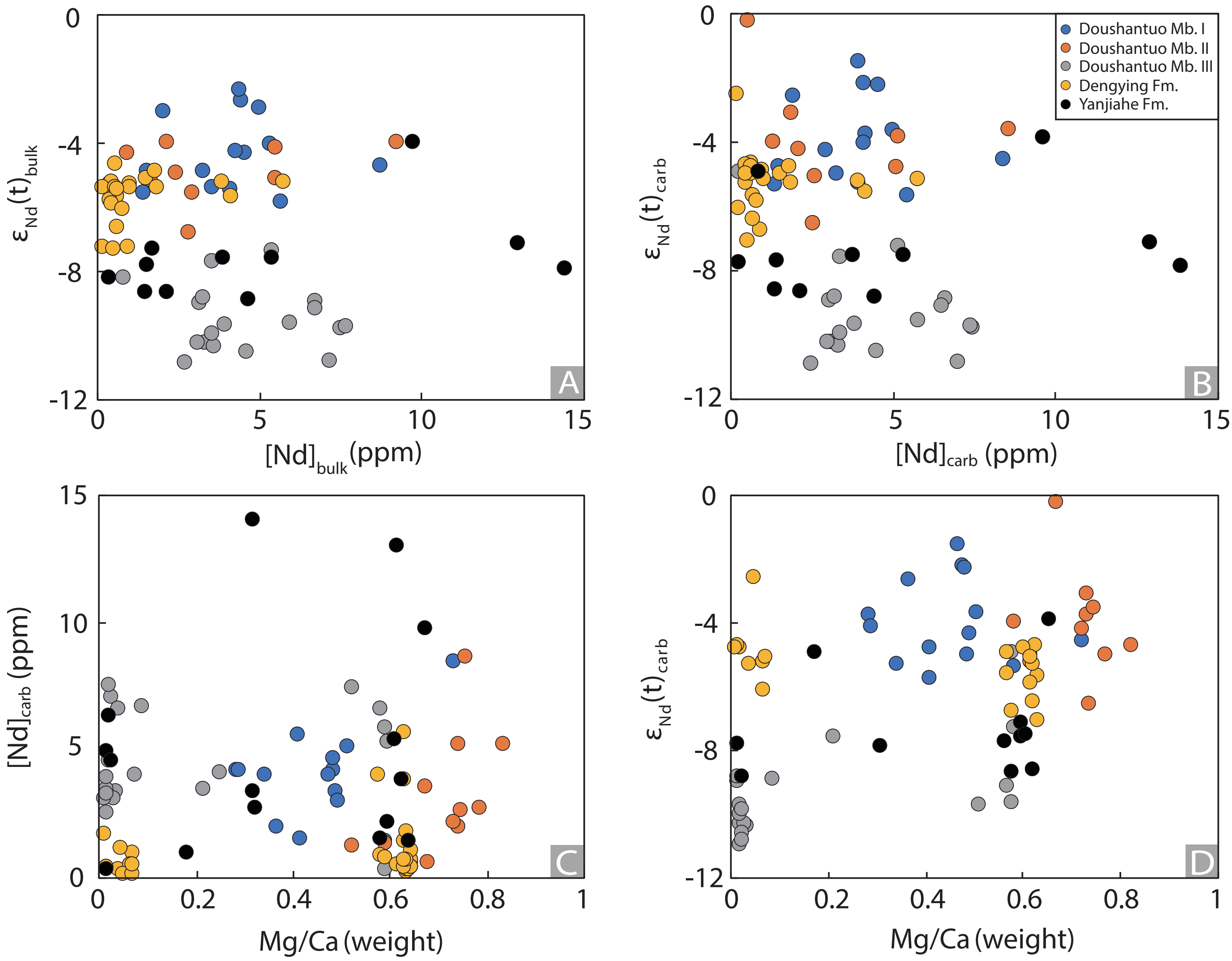
A
B
C
D
$\varepsilon_{Nd}(t)_{bulk}$
$[Nd]_{bulk}$ (ppm)
$\varepsilon_{Nd}(t)_{carb}$
$[Nd]_{carb}$ (ppm)
Mg/Ca (weight)
Doushantuo Mb. I
Doushantuo Mb. II
Doushantuo Mb. III
Dengying Fm.
Yanjiahe Fm.

Figure 5

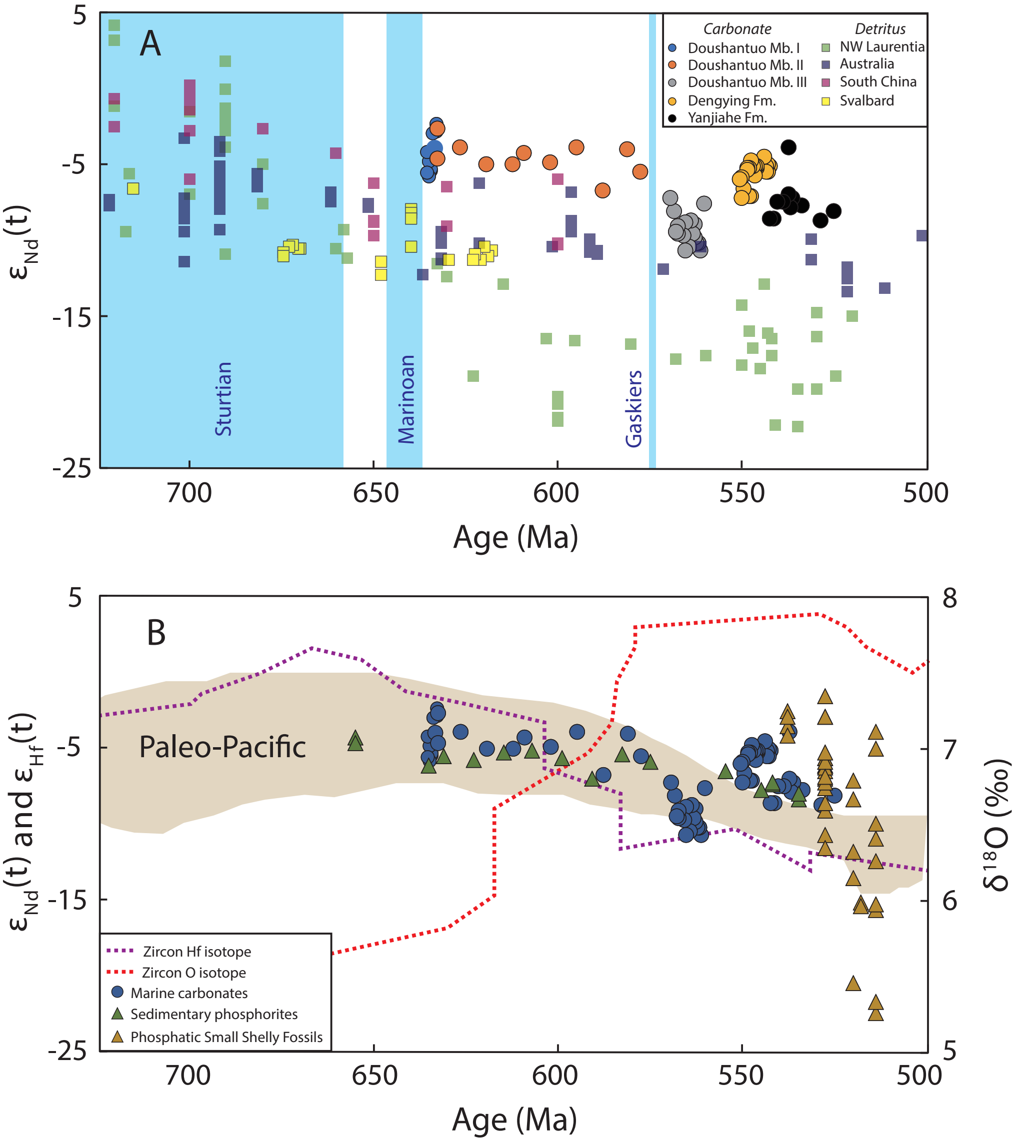

A
Carbonate
Doushantuo Mb. I
Doushantuo Mb. II
Doushantuo Mb. III
Dengying Fm.
Yanjiahe Fm.
Detritus
NW Laurentia
Australia
South China
Svalbard
Sturtian
Marinoan
Gaskiers
$\varepsilon_{Nd}(t)$
Age (Ma)
B
Paleo-Pacific
Zircon Hf isotope
Zircon O isotope
Marine carbonates
Sedimentary phosphorites
Phosphatic Small Shelly Fossils
$\varepsilon_{Nd}(t)$ and $\varepsilon_{Hf}(t)$
$\delta^{18}O$ (‰)
Age (Ma)

Figure 6

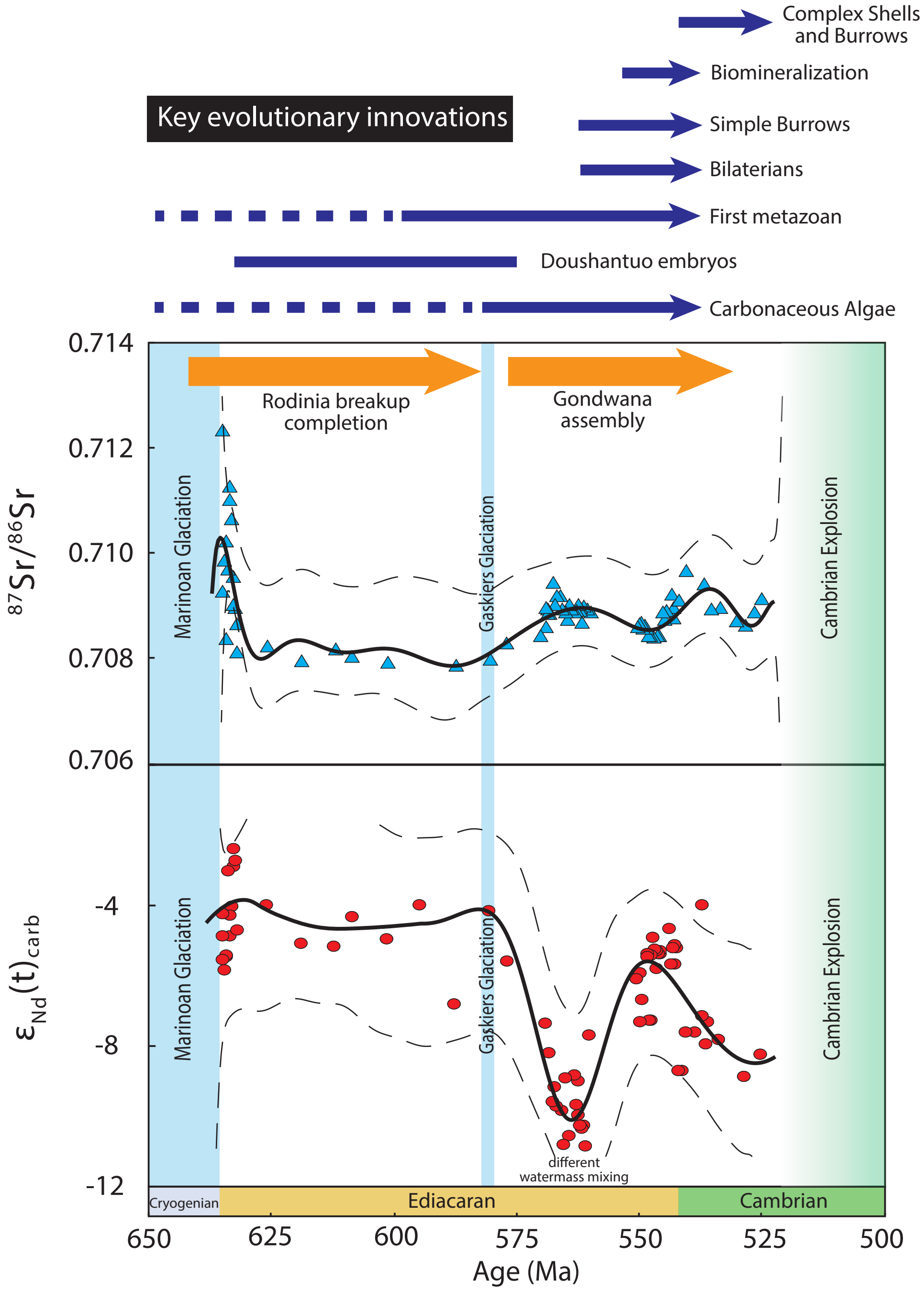
Complex Shells and Burrows
Biomineralization
Key evolutionary innovations
Simple Burrows
Bilaterians
First metazoan
Doushantuo embryos
Carbonaceous Algae
0.714
0.712
0.710
0.708
0.706
$^{87}Sr/^{86}Sr$
Rodinia breakup completion
Gondwana assembly
Marinoan Glaciation
Gaskiers Glaciation
Cambrian Explosion
-4
-8
-12
$\varepsilon_{Nd}(t)_{carb}$
different watermass mixing
Cryogenian
Ediacaran
Cambrian
650
625
600
575
550
525
500
Age (Ma)

Figure 7